scientific reports

Check for updates

OPEN

Clinical value and radiographic features of low dose CT scans compared to X rays in diagnosing mycoplasma pneumonia in children

Simin Xiao[1,3], Siyuan Zeng[2,3] & Yangbin Kou[1]✉

The aim of this article is to explore the lung characteristics and diagnostic value of X-ray and low-dose computed tomography (LDCT) in children with mycoplasma pneumoniae pneumonia (MPP). A total of 807 suspected children with MPP admitted to outpatient and inpatient departments from August 2023 to November 2023, were selected and divided into X-ray group ($n = 389$) and LDCT group ($n = 418$) according to the examination method. The two groups received chest X-ray examination and LDCT examination, respectively. Using pathogen detection results as the gold standard, we compared the imaging visible symptoms, diagnostic rate, sensitivity, specificity, diagnostic accuracy, and missed diagnosis rate of the two examination methods. In the LDCT, the main manifestations were thickened lung markings, patchy and striped shadows, followed by ground glass-like shadows, interstitial infiltration of the lungs, tree-in-fog sign, bronchial wall thickening, pleural thickening, consolidation/atelectasis, air bronchogram sign, and branching linear opacities (tree-in-bud sign). The main manifestations of X-ray were thickening of lung markings, followed by pulmonary patchy shadows, interstitial infiltration, and consolidation/atelectasis. LDCT scans revealed 359 cases of pediatric MPP, with 337 true positives cases, 22 false negatives cases, 23 false positives cases, and 36 true negatives cases. On the other hand, X-ray examinations identified 308 cases of pediatric MPP, with 266 true positive cases, 42 false negative cases, 35 false positive cases, and 46 true negative cases. The diagnostic rate, sensitivity, specificity and diagnostic accuracy of LDCT scans were 80.62%, 93.87%, 61.02% and 89.23%, which were higher compared to X-ray examinations, with the values of 68.38%, 86.36%, 56.79% and 80.21%. The missed diagnosis rate for LDCT was 6.13%, which was lower than the 13.64% rate for X-ray. LDCT demonstrated higher visibility of diagnostic rate, sensitivity, specificity and diagnostic accuracy compared to X-ray examinations, and the missed diagnosis rate of LDCT was lower than that of X-ray. Additionally, the radiographic features of LDCT were more characteristic, with simpler procedure, greater clinical utility.

Keywords Low-dose computed tomography, Chest X-ray, Mycoplasma pneumoniae pneumonia in children, Diagnostic value, Radiographic features

Mycoplasma pneumoniae pneumonia (MPP) is an acute pulmonary inflammation caused by mycoplasma pneumoniae (MP) infection that is commonly found in the respiratory system of children. MPP is often accompanied by atelectasis and extensive pulmonary infiltration leading to extrapulmonary complications. MP is one of the main pathogens causing community-acquired pneumonia in children. MP infection is also a pathogen of respiratory tract infections in infants and young children, and it clinically presents mostly as respiratory tract infection syndrome, with approximately 3–10% developing into MPP. Although MPP is usually self-limiting, it can lead to complications and even endanger life[1]. The clinical manifestations include persistent fever even with early standardized use of antibiotics, no relief of cough and asthma symptoms, and even worsening imaging signs. The condition may progress to refractory MPP and is often accompanied by pulmonary and extrapulmonary complications, causing damage to multiple organ systems. In recent years, there has been a gradual increase in refractory MPP cases[2]. Therefore, using imaging methods to accurately

[1]Radiology department, The First Affiliated Hospital of Traditional Chinese Medicine of Chengdu Medical College, XinDu Hospital of Traditional Chinese Medicine, Chengdu, China. [2]Department of Obstetrics and Gynecology, West China Second University Hospital, Sichuan University, Chengdu, China. [3]These authors contributed equally: Simin Xiao and Siyuan Zeng. ✉email: 1340305847@qq.com

identify and detect childhood MPP is of great significance for its early diagnosis. In recent years, imaging examinations have been used in the diagnosis and treatment of pneumonia. Their value is increasing, and the range and morphology of lung lesions in children can be observed in a timely manner, thus providing reliable basis for clinical treatment. At present, the most commonly used diagnostic methods for MPP infection in children include X-ray examination and computed tomography (CT) examination in clinical practice. However, X-ray examination images show relatively few symptoms, which can easily lead to missed diagnosis[3]. Spiral CT scanning has high density resolution and spatial resolution, which can clearly display lung lesions in children[4]. However, it is worth noting that if conventional spiral CT scanning radiation dose is applied, it may increase family concerns and reduce the compliance of pediatric examinations. Therefore, it is clinically recommended to effectively control the dose of spiral CT scanning. In recent years, with the continuous development of medical technology, imaging technology, and the continuous improvement of instrument equipment and reconstruction technology, low-dose computed tomography (LDCT) technology has been applied in diagnosing most lung diseases[5]. To determine the most suitable diagnostic method, this article focuses on 807 children with MPP admitted to our hospital, aiming to explore the clinical effects of LDCT scanning and X-ray examination in the diagnosis of MPP in children.

Materials and methods

General information

A total of 807 suspected children with MPP admitted to the outpatient and inpatient departments from August 2023 to November 2023 were selected. LDCT and X-ray examinations were conducted voluntarily by the patients and their families, including 427 males and 380 females. According to the examination method, they were divided into X-ray group ($n=389$) and LDCT group ($n=418$). The patients' age range was from 3 months to 12 years old, with an average age of (5.47 ± 2.39) years in the X-ray group and (5.24 ± 2.72) years in the LDCT group. There were no statistically significant differences in the general characteristics, such as gender and age of the patients ($P>0.05$) (See Table 1). The clinical manifestations of all patients were mainly fever and cough, which may be accompanied by headache, runny nose, sore throat, ear pain, etc. All patients met the diagnostic criteria of the Diagnosis and Treatment Guidelines for Mycoplasma Pneumonia in Children (2023 edition). This study has been approved by the Ethics Committee of the First Affiliated Traditional Chinese Medicine Hospital of Chengdu Medical College (Sichuan, China) and all experiments were performed in accordance with relevant guidelines and regulations.

Inclusion and exclusion criteria

Inclusion criteria: (1) All patents were aged at 3 months-12 years; (2) The main clinical manifestations that met the clinical diagnostic criteria included cough, fever, loss of appetite, and moist rales in the lungs; (3) All patients passed the following criteria: ① Children with positive (+) result of serum MP-IgM antibody (diluted 1 : 160) diluted using particle agglutination method; During the course of the disease, the titers of double serum MP antibodies increased by 4 times or more. ② the constant temperature amplification method was used to measure the nucleic acid of mycoplasma for ribonucleic acid quantitative detection, and any one or both of the above items were combined to diagnose MPP positive or negative; (4) informed consent was obtained from all subjects and/or their legal guardian(s).

Exclusion criteria: (1) Individuals with mental disorders; (2) Individuals with severe organic diseases; (3) Individuals with missing clinical data; (4) Family members who understood the purpose of this study but refuse participation.

Inspection methods

(1) X-ray examination: The child maintained a standing or supine position and used an X-ray detector (brand: Siemens, model: Ysio) to scan multiple parts of the child's mediastinum, pleura, chest, etc. The exposure value and conditions were adjusted according to the thickness of patients' body, and the target film distance was set to 100–150 cm. (2) LDCT scanning examination: All examinations were performed using a 40-row spiral LDCT scanning scheme (brand: co imaging, model: uCT 528), with the scanning position in supine position, head advanced, and the scanning range from the chest entrance to the lung bottom. The tube voltage was 120 kV, and the tube current used automatic milliampere second technology. The scanning layer thickness and spacing were both 5 mm, and the image reconstruction layer was 1.2 mm. The field of view was set to a small body, with a pitch of 1.15:1, a rotation time of 0.75 s, and a collimation width of 22 mm. The imaging matrix was 512×512. The mediastinal window settings were a width of 400 and a level of 40, while the lung window settings were a width of 1400 and a level of −400. Based on clinical diagnostic needs, sagittal and coronal reconstruction were performed on the lesion area. After the scanning was completed, all image data were uploaded to the 3D workstation, and both examination results were evaluated by professional imaging physicians.

Clinical data		Low-dose CT group	X-ray group	$\chi2$ /Z	*P*
Gender	Male	221	206	0.001	0.981
	Female	197	183		
Age		5.47±2.39	5.24±2.72	−1.86	0.063

Table 1. Clinical data of children in the low-dose CT and X-ray groups.

Observation indicators

(1) The results of LDCT and X-ray imaging examinations were analyzed. Comparing the imaging findings of the two groups, the visible symptoms included thickened lung markings, patchy and striped shadows, air bronchogram sign, interstitial infiltration of the lungs, ground glass-like shadows, pleural thickening, bronchial wall thickening, branching linear opacities (tree-in-bud sign), and tree-in-fog sign. (2) The imaging characteristics of the two examination methods were compared, serum examination (particle agglutination method) and ribonucleic acid quantitative detection were used as the gold standard, and the diagnosis rates of the two examination methods were analyzed. (3) Using the results of pathogen testing as the gold standard, the sensitivity, specificity, diagnostic accuracy, and missed diagnosis rate of the two examination methods were calculated.

Statistical methods

Statistical analysis was implemented based on SPSS 26.0 software. Specifically, it included: ① if the quantitative data conformed to a normal distribution and homogeneity of variance, the mean ± standard deviation (± s) was used to describe it. An independent sample t-test was used for inter group comparison, and a paired sample t-test was used for intra group comparison; ② If it did not follow a normal distribution, it was described using the median and interquartile spacing [M (P25, P75)], and a paired sample rank sum test was used for intragroup comparison, while an independent sample rank sum test was used for intergroup comparison. ③ The counting data was described using frequency (composition ratio) and chi square was used(χ 2) Inspection; ④ $P<0.01$ indicated a significant statistical difference, while $P<0.05$ indicated a statistical difference. All numbers were rounded to two decimal places.

Results

LDCT examination results

LDCT scan chest results mainly showed thickened lung markings and patchy and striped shadow, accounting for 78.23% (327/418). The second most common finding was ground glass-like shadows, followed by interstitial infiltration of the lungs (Fig. 1), tree-in-fog sign (Fig. 2), bronchial wall thickening, pleural thickening, consolidation/atelectasis, air bronchogram sign (as shown in Fig. 3), and branching linear opacities (tree-in-bud sign) (Fig. 4). See Table 2.

X-ray examination results

The main manifestation of chest X-ray examination was a thickened lung markings, accounting for 75.58% (294/389), followed by patchy and striped shadows, interstitial infiltration (Fig. 5), and consolidation/atelectasis (Fig. 6). See Table 3.

Diagnostic results of LDCT scan examination and x-ray examination

Pathogen detection results showed that among 807 suspected cases of pediatric MPP, 667 tested positive and 140 tested negative. LDCT scan examination results showed 337 true positive cases, 22 false negative cases, 23 false positive cases, and 36 true negative cases. X-ray examination results showed 266 true positive cases, 42 false negative cases, 35 false positive cases, and 46 true negative cases (Table 4). The diagnosis rate of MPP in the LDCT group was significantly higher than that in the X-ray group, with a statistically significant difference ($P<0.01$) (Table 5).

Fig. 1. Shows a fine grid like high-density shadow with thickened interstitial tissue in the lobules.

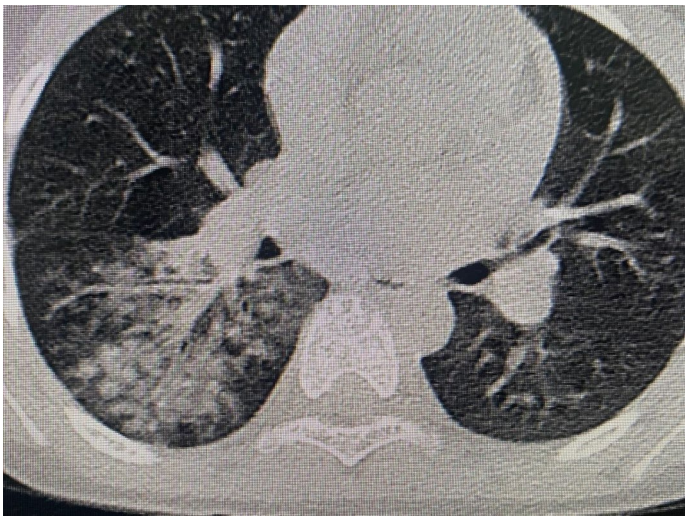

Fig. 2. Tree-in-fog sign: In the blurred ground glass-like shadows, acinar nodules can be seen, which are blurry and thicker than the branching linear opacities (tree-in-bud sign).

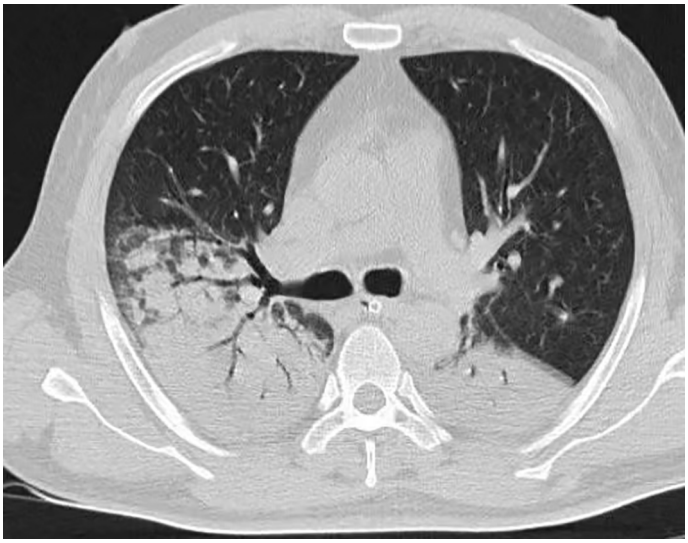

Fig. 3. Involves lung parenchyma and presents with segmental atelectasis, characterized by consolidation/atelectasis. The long axis of consolidation aligns with the direction of the bronchi, and an air bronchogram is visible inside.

Comparison of sensitivity, specificity, diagnostic accuracy and missed diagnosis rate between LDCT and x-ray examinations

Using clinical serum tests and RNA as the gold standard, the sensitivity of LDCT in diagnosing pediatric MPP was 93.87%, and the diagnostic accuracy was 89.23%, and the two values were significantly higher than those of X-ray, which were 86.36% and 80.21%, respectively, with statistically significant difference ($P<0.05$). The specificity of LDCT in diagnosing pediatric MPP was 61.02%, which was higher than that of X-ray (56.79%), but the difference was not statistically significant ($P>0.05$). The missed diagnosis rate for LDCT was 6.13%, which was lower than that of the X-ray (13.64%), with statistically significant difference ($P<0.05$) (Table 6).

To evaluate the diagnostic accuracy of low-dose CT (LDCT) and chest X-ray, we plotted the AUC-ROC curve (Fig. 7)

The results showed that the AUC value of LDCT was 0.774, while the AUC value of chest X-ray was 0.716, which indicated that low-dose CT is superior to chest X-ray in terms of diagnostic accuracy, with higher sensitivity and specificity.

Fig. 4. Thickening of the bronchial tube wall, narrowing of the lumen, and formation of a branching linear opacities (tree-in-bud sign) with mucus plugs in the bronchioles.

Low-dose CT imaging features	Number	Proportion
Patchy and striped shadows	327	78.23%
Thickened lung markings	327	78.23%
Ground glass-like shadows	238	56.94%
Interstitial infiltration	198	47.37%
Tree-in-fog sign	192	45.93%
Bronchial wall thickening	191	45.69%
Pleural thickening	177	42.34%
Consolidation/atelectasis	166	39.71%
Air bronchogram	121	28.95%
Tree-in-bud sign	68	16.27%

Table 2. Imaging features observed in low-dose CT scans for diagnosing Mycoplasma pneumonia in children.

Discussion

As a type of microorganism that lies between viruses and bacteria, MP is rarely found in the alveoli and mainly transmitted through droplets. The incubation period is 2–3 weeks, and the infection primarily affects the epithelial cells lining the trachea to the respiratory bronchioles. Once adhered to these epithelial cells, MP can lead to ciliary dysfunction, causing swelling in the walls of the small bronchi and trachea. Additionally, it can affect the interstitium around lymphatic vessels and blood vessels. In severe cases, it can result in the formation of mucous plugs within the airways, leading to cardiovascular, hematological, and central nervous system dysfunction. Some individuals may also develop otitis media, which can significantly impact the growth and development of children, so early detection and treatment are crucial. The pathological changes of MPP are mainly interstitial pneumonia, and sometimes they are accompanied by bronchopneumonia, usually only mild respiratory symptoms such as headache, sore throat, fever, cough, etc[6]. With the aggravation of environmental pollution and industrial pollution, the incidence rate of MPP has gradually increased, especially in the three seasons of spring, autumn and summer, and the incidence rate is quite high. Due to their poor resistance, children are prone to infection, thereby leading to an increasing probability of this disease[7].

Early X-ray manifestations of MPP patients include thickened lung markings, interstitial pneumonia, and reticular shadows, while later X-ray manifestations include uniform speckled, reticular, and ground glass-like shadows. This may be due to the decreased transparency of the lung lobes on imaging after mycoplasma infection and the loss of gas in the alveoli caused by a large amount of inflammatory exudation. As a result, large dense shadows appear in the lungs, which masks their interstitial changes[8]. On X-ray, specific manifestations of MPP infection include small patchy, and dense shadows in the perihilar and pericardial regions. These are often found in the lower lobes of both lungs, with blurred margins. Interstitial infiltrates, accompanied by an enlargement of the pulmonary hilum, are observed extending from the cardiac silhouette to the pulmonary hilar regions.

In this study, after X-ray examination, the results proved that the chest manifestations of the patients were varied, mainly divided into thickened lung markings, patchy and striped shadows, interstitial infiltration, and consolidation/atelectasis in 294, 257, 141, and 45 cases, respectively. Among LDCT patients, 327 cases showed

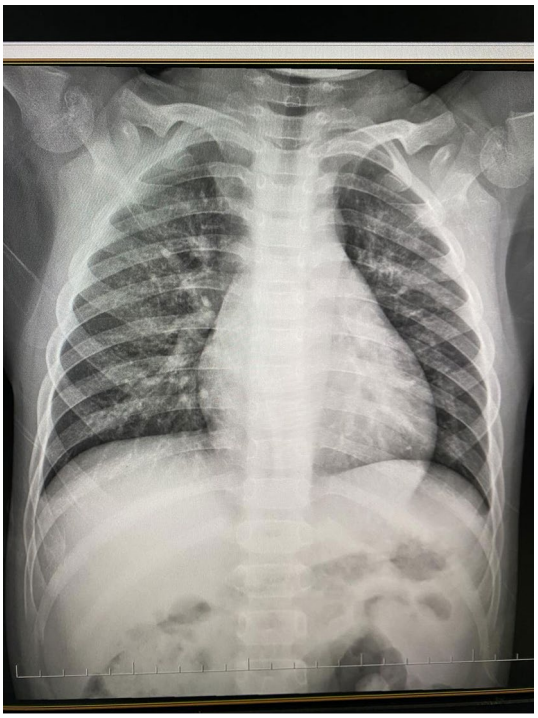

Fig. 5. Shows that the lung markings have become more numerous and thickened, often presenting as grid like and cord like shadows. The bronchial wall has thickened, with blurred edges and reduced local transparency.

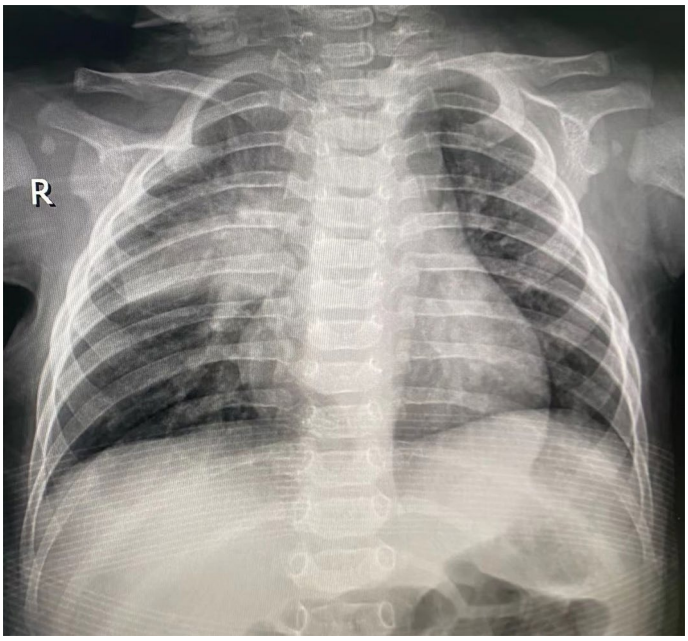

Fig. 6. Shows a leaf shaped high-density consolidation shadow on the upper right lung, with uneven density and blurred edges. homogenous dense opacity in at least one lobe, with or without an air-bronchogram in the lesion.

thickened lung markings and patchy and striped shadows, 238 cases of ground glass-like shadows, 198 cases of interstitial infiltration in the lungs, 192 cases of tree-in-fog sign, 191 cases of bronchial wall thickening, 177 cases of pleural thickening, 166 cases of consolidation/atelectasis, 121 cases of air bronchogram sign, and 68 cases of branching linear opacities (tree-in-bud sign). X-ray examination revealed that the patients often presented with segmental parenchymal and interstitial infiltration, with less extensive infiltration and solid

X-ray imaging features	Number	Total	Proportion
Thickened lung markings	294	389	75.58%
Patchy and striped shadows	257	389	66.07%
Interstitial infiltration	141	389	36.25%
Consolidation/atelectasis	45	389	11.57%

Table 3. Imaging features observed in X-rays for diagnosing Mycoplasma pneumonia in children.

Diagnostic method	Types	Pathogenic results	
		Diagnosis	Undiagnosed
Low-dose ct	Diagnosis	337	23
	Undiagnosed	22	36
X-ray	Diagnosis	266	35
	Undiagnosed	42	46

Table 4. Comparison of diagnostic results between low-dose CT and X-rays for Mycoplasma pneumonia in children.

Group	Number of cases	Number of cases of MPP	Diagnosis rate of Mycoplasma pneumonia/%	χ2	*P*
Low-dose CT group	418	337	80.62%	15.99	0
X-ray	389	266	68.38%		

Table 5. Comparison of the diagnostic rates of low-dose CT and X-rays for Mycoplasma pneumonia in children.

Group	Sensitivity	Specificity	Accuracy	Missed diagnosis rate
Low-dose CT Group	93.87%	61.02%	89.23%	6.13%
X-ray	86.36%	56.79%	80.21%	13.64%
χ^2	10.773	0.251	12.8	10.773
P	0.001	0.616	0	0.001

Table 6. Comparison of diagnostic sensitivity, specificity, accuracy, and missed diagnosis rates between low-dose CT and X-rays for Mycoplasma pneumonia in children.

changes. Some children had enlarged lymph nodes in the hilum of the lungs, while a few had pleural effusion[9]. The visible symptoms obtained from X-ray examination are relatively few. As a common imaging examination method, LDCT can clearly reflect the pulmonary parenchymal lesions and interstitial conditions in children with MPP. After MPP infection, the initial lesions occur in the ciliated epithelium. As inflammation progresses to the alveoli, it leads to exudation within the alveolar spaces. Subsequently, the exudate spreads along the bronchovascular bundles and gradually expands and reaches the alveoli, thus causing parenchymal lung lesions. This dual mechanism accounts for the presence of both interstitial pneumonia features and parenchymal lesions in MPP. Specifically, nodular opacities distributed centrally within the lobules and thickening of interlobular septa can be observed on imaging. In this study, LDCT mainly showed thickened lung markings and patchy and striped shadows in the lungs of children with MPP. When the bronchial wall is swollen and thickened, and the lumen is narrowed, mucus embolism would appear in the bronchioles, forming a "tree-in-bud sign" on CT. When it spreads to the surrounding interstitium, congestion, edema, and inflammatory cell infiltration would develop in the lung interstitium, forming a "tree mist sign" on CT. The overall manifestation is low density, with blurred edges, cloud-like, ground glass-like shadows, and cloud-like shadows distributed from the hilum to the periphery of the lungs. Inflammatory lesions in the pulmonary interstitium can also lead to alveolar lesions, ultimately reaching the alveolar parenchyma and causing pulmonary parenchymal lesions. Large areas of consolidation shadows appear, and the long axis of consolidation can be clearly observed on CT images, which is consistent with the shape of the bronchi, without necrosis, and with rare cavities. On the one hand, CT can clearly show thickening of the bronchial wall and narrowing of the lumen caused by inflammatory infiltration of the bronchi. On the other hand, pulmonary atelectasis is more pronounced due to the obstruction of small airways by inflammatory exudates. Compared with X-ray examination, LDCT examination has a higher value in identifying bronchitis, mixed pathological changes, and interstitial pneumonia[8].

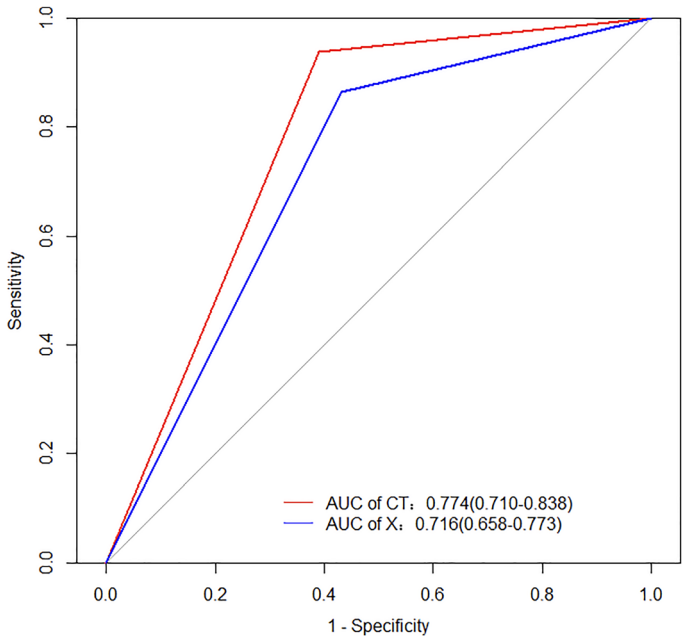

Fig. 7. AUC-ROC curves comparing the diagnostic performance of low-dose CT and X-rays in detecting Mycoplasma pneumonia in children.

This study also revealed that DLCT examination has higher diagnostic rate, sensitivity, specificity and diagnostic accuracy in diagnosing MPP in children, compared to X-ray examination. CT has high resolution and is easy to display small lesions, thus making it more accurate than ordinary X-ray examinations. At the same time, it can avoid missed diagnosis for the overlapping physiological and anatomical structures[10]. However, clinical practice has indicated that the radiation dose for conventional CT scans is usually 8–9 times higher than that of LDCT radiation, and far higher than X-ray detection and LDCT examination[11], which poses a potential threat to human health, especially for the younger age group. Some studies have illustrated that the increased radiation risk of children under 10 years old is more obvious[12]. The incidence rate of tumors is highly related to the CT radiation received in childhood[13]. It is an important problem that needs to be solved urgently to reasonably reduce the radiation dose of children on the premise of ensuring the needs of diagnosis and treatment. Therefore, low dose scanning technology has gained widespread attention[14,15]. Methods for reducing CT radiation dose include increasing scanning pitch, reducing tube voltage and tube current, and applying automatic tube current regulation technology[16,17]. At the same time, image quality can be improved in the original algorithm stage to meet the clinical diagnostic requirements of images, and a large number of literature has confirmed that this method is effective[18–21]. This study selected tube voltage based on the age of the patient, and used Dose Right automatic tube current exposure control technology for tube current. KARL 3D iterative noise reduction algorithm was used to reduce 65% of image noise, which can also reduce scanning conditions. This study indicates that according to scanning parameters, patients weighing less than 20 kg absorb approximately 0.4–0.7 mSv of radiation that was equivalent to a dose of 4–8 chest X-rays, while patients weighing 20–60 kg absorb approximately 0.7–1.5 mSv that was equivalent to a dose of 7–16 chest X-rays[22], which is much smaller than the radiation dose that may increase the risk of cancer. LDCT offers several advantages in diagnosing MPP :1. It has the advantages of clear image display, clear anatomical relationships, complete lesion display, high sensitivity, and specificity, which means that even mild lung inflammation can be accurately identified by low-dose chest CT. This is crucial for timely diagnosis and treatment of pneumonia, especially for children, a high-risk group. 2. Rapid Imaging: LDCT scans can be completed quickly, which is particularly beneficial for children. This translates to shorter examination times, thus reducing the need for them to remain sedated and improving the success rate of the examination. 3. Lower Radiation Dose: Compared to conventional CT scans, LDCT employs a lower radiation dose. This is especially crucial in children, who are more sensitive to radiation. Reducing radiation exposure helps mitigate potential long-term health risks. 4. Cost savings: Low dose CT technology reduces unnecessary radiation exposure and repetitive examinations, which could help reduce the medical costs. At the same time, it reduces the wear and tear of the X-ray tube, extends the service life of the tube, and saves costs.

We are fully aware that the routine use of CT scans may increase the risk of radiation exposure and also bring higher costs. In most MPP cases, X-rays can provide sufficient preliminary diagnostic information, so it is not advisable to routinely use CT scans for all suspected MPP cases. The indications for CT examination should be determined based on the specific clinical context. To balance the benefits and potential risks of CT use, we recommend adopting a stratified screening strategy in clinical practice. In most common MPP cases, X-rays can serve as a preliminary diagnostic tool. However, for patients with atypical clinical symptoms or imaging results that do not match clinical manifestations, CT scans can serve as a further confirmation tool. Especially

in immunocompromised populations, children, the elderly, or other high-risk groups, we tend to use CT scans to detect potential complications or subtle lung lesions as early as possible, aiming to ensure timely intervention and avoid worsening the condition. In some patients with suspected complications or severe disease course, if there is clinical suspicion of complications (such as lung consolidation, pleural effusion, etc.), or if symptoms persist, CT can more effectively evaluate the actual extent of lung lesions and provide guidance for further treatment. Future research should focus on evaluating the clinical value of CT scanning in MPP diagnosis, especially in terms of radiation risk and economic benefits of low-dose CT. Further research can explore the frequency of CT use and its impact on clinical outcomes in patients with different risk groups and develop more accurate diagnostic pathways to ensure that the use of CT can improve diagnostic accuracy while reasonably controlling radiation exposure and costs.

This study has several strengths:1. Large Sample Size: The study included 807 suspected cases of MPP, which is a relatively large sample size, which could enhance the reliability and representativeness of the research results. 2. Comparative Analysis: The paper employed a comparative analysis approach, comparing X-ray and LDCT scans, which helps assess their advantages and disadvantages in diagnosing MPP. 3. Pathogen Detection as Gold Standard: The study used pathogen detection results as the gold standard, aiming to ensure diagnostic accuracy and enhance the credibility of the research findings. 4. Comprehensive Evaluation of Radiographic Features: The paper provided a detailed description of the radiographic features of X-ray and LDCT scans in diagnosing MPP, including lung texture, patchy shadows, and linear shadows, which offers readers a comprehensive understanding. 5. Clear Results: The study yielded clear and definite results, which indicated that LDCT scans outperformed X-ray examinations in terms of diagnostic accuracy and sensitivity for MPP, and this could provide robust support for clinical practice.

Our research has certain shortcomings. Firstly, this study is a retrospective study, so the analysis is limited to existing medical records and lacks a certain degree of foresight. Retrospective design is difficult to avoid partial bias, especially the subjective interpretation of imaging results by radiologists. The current study did not implement blinding due to limitations such as design conditions and data availability. However, the study minimized the error by multiple verifications of imaging results and expert collaboration. Future research should consider having radiologists interpret images without knowledge of patients' clinical background or conducting independent blinded evaluations by multiple radiologists to reduce potential bias. Due to the severity of symptoms, patients could choose the type of examination, and thus a significant difference in sample size between the two formed, which may lead to systematic differences between the two groups in imaging manifestations, disease severity, clinical manifestations, and other aspects. Therefore, selection bias may affect the comparison of results between two groups, especially in the assessment of diagnostic accuracy or disease progression. We suggest that future studies adopt randomized controlled trials (RCTs) or prospective designs to reduce the risk of selection bias and obtain more reliable results. Secondly, the imaging examination results of LDCT and X-ray are greatly affected by their scanning time. Although all participants in this study received CT and X-ray scans within 24 h after admission, it cannot be guaranteed that all patients' CT and X-ray images were obtained in the same disease stage. If conditions permit, the inclusion of patients should be limited to the same stage of their illness, and the CT and X-ray scanning times of the two groups of patients should be statistically calculated to reduce bias and concretize results. Moreover, in the paper, we did not explicitly discuss the potential impact of confounding factors on the results. Especially, some factors, such as the severity of the disease, patients' basic health status, or past treatment history, may affect the selection of imaging examinations (such as CT or X-ray) and diagnostic results. Future research can adopt a prospective design and systematically evaluate and control for all potential confounding factors at the beginning of the study, which can help further improve the reliability and external validity of the results.

In our study, although clinical diagnosis typically relies on symptoms, laboratory data, and imaging results, we believe that radiological confirmation plays an important role in diagnosing pneumonia types, particularly MPP. The clinical manifestations of MPP are often similar to other types of pneumonia, and the symptoms are not always specific, so imaging examinations play a crucial complementary role in diagnosis. Through radiological confirmation, different types of pneumonia can be more effectively distinguished, thus helping to rule out other possible causes, such as bacterial pneumonia or viral pneumonia, and guiding the selection of treatment plans. Especially, LDCT that provides more accurate images of lung lesions has significant advantages in early detection and diagnosis of mycoplasma pneumonia, which could provid added value for clinical doctors' diagnosis and help make more accurate diagnoses in clinical practice.

Conclusion

In summary, both LDCT scans and X-ray imaging played important roles in the early diagnosis of MPP in children. LDCT demonstrated higher visibility of diagnostic rate, sensitivity, specificity and diagnostic accuracy compared to X-ray examinations, and its missed diagnosis rate was lower than that of X-ray. Additionally, the radiographic features of LDCT were more characteristic, with simpler procedure and greater clinical utility.

Data availability

The research data supporting the results of this manuscript are available upon reasonable request. The data sets generated and analyzed during the current study are not publicly available due to [specific reasons, e.g., privacy, ethical restrictions] but are available from the corresponding author on reasonable request.For data requests, please contact Yangbin Kou at 1340305847@qq.com.

Received: 29 June 2024; Accepted: 11 March 2025
Published online: 17 March 2025

References

1. Lee, Y. C. et al. Altered chemokine profile in refractory Mycoplasma pneumoniae pneumonia infected children. *J. Microbiol. Immunol. Infect. = Wei Mian Yu Gan Ran Za Zhi.* **54**, 673–679. https://doi.org/10.1016/j.jmii.2020.03.030 (2021).
2. Zhao, F. et al. Antimicrobial susceptibility and molecular characteristics of Mycoplasma pneumoniae isolates across different regions of China. *Antimicrob. Resist. Infect. Control.* https://doi.org/10.1186/s13756-019-0576-5 (2019).
3. Reittner, P. et al. Mycoplasma pneumoniae pneumonia: radiographic and high-resolution CT features in 28 patients. *AJR Am. J. Roentgenol.* **174**, 37–41. https://doi.org/10.2214/ajr.174.1.1740037 (2000).
4. Wang, J., Xia, C., Sharma, A., Gaba, G. S. & Shabaz, M. Chest CT findings and differential diagnosis of Mycoplasma pneumoniae pneumonia and Mycoplasma pneumoniae combined with Streptococcal pneumonia in children. *J. Healthc. Eng.* https://doi.org/10.1155/2021/8085530 (2021).
5. Tækker, M., Kristjánsdóttir, B., Graumann, O., Laursen, C. B. & Pietersen, P. I. Diagnostic accuracy of low-dose and ultra-low-dose CT in detection of chest pathology: a systematic review. *Clin. Imaging.* **74**, 139–148. https://doi.org/10.1016/j.clinimag.2020.12.041 (2021).
6. Rodman Berlot, J. et al. Clinical characteristics of infections caused by Mycoplasma pneumoniae P1 genotypes in children. *Eur. J. Clin. Microbiol. Infect. Diseases: Official Publication Eur. Soc. Clin. Microbiol.* **37**, 1265–1272. https://doi.org/10.1007/s10096-018-3243-5 (2018).
7. Yamasaki, K. et al. Successful additional corticosteroid treatment in a patient with Mycoplasma pneumoniae pneumonia in whom a monobacterial infection was confirmed by a molecular method using Bronchoalveolar lavage fluid. *Intern. Med. (Tokyo, Japan).* **55**, 703–707. https://doi.org/10.2169/internalmedicine.55.5124 (2016).
8. Gong, L., Zhang, C. L. & Zhen, Q. Analysis of clinical value of CT in the diagnosis of pediatric pneumonia and Mycoplasma pneumonia. *Experimental Therapeutic Med.* **11**, 1271–1274. https://doi.org/10.3892/etm.2016.3073 (2016).
9. Zhou, F. J. et al. Diagnostic value of analysis of H-FABP, NT-proBNP, and cTnI in heart function in children with congenital heart disease and pneumonia. *Eur. Rev. Med. Pharmacol. Sci.* **18**, 1513–1516 (2014).
10. W Goldman, L. Principles of CT and CT technology. *J. Nucl. Med. Technol.* **35**, 115–128. https://doi.org/10.2967/jnmt.107.042978 (2007). quiz 129–130.
11. Kang, Z., Li, X. & Zhou, S. Recommendation of low-dose CT in the detection and management of COVID-2019. *Eur. Radiol.* **30**, 4356–4357. https://doi.org/10.1007/s00330-020-06809-6 (2020).
12. Chodick, G., Ronckers, C. M., Shalev, V. & Ron, E. Excess lifetime cancer mortality risk attributable to radiation exposure from computed tomography examinations in children. *Isr. Med. Association Journal: IMAJ.* **9**, 584–587 (2007).
13. Priyanka, Kadavigere, R., Sukumar, S. & Pendem, S. Diagnostic reference levels for computed tomography examinations in pediatric population - A systematic review. *J. Cancer Res. Ther.* **17**, 845–852. https://doi.org/10.4103/jcrt.JCRT_945_20 (2021).
14. Wu, D., Wang, G., Bian, B., Liu, Z. & Li, D. Benefits of Low-Dose CT scan of head for patients with intracranial hemorrhage. *Dose-response: Publication Int. Hormesis Soc.* **19**, 1559325820909778. https://doi.org/10.1177/1559325820909778 (2020).
15. Duffy, S. W. & Field, J. K. Mortality reduction with Low-Dose CT screening for lung cancer. *N. Engl. J. Med.* **382**, 572–573. https://doi.org/10.1056/NEJMe1916361 (2020).
16. Park, M. S., Ha, H. I., Ahn, J. H., Lee, I. J. & Lim, H. K. Reducing contrast-agent volume and radiation dose in CT with 90-kVp tube voltage, high tube current modulation, and advanced iteration algorithm. *PloS One.* **18**, e0287214. https://doi.org/10.1371/journal.pone.0287214 (2023).
17. Lee, J. et al. Diagnostic accuracy of low-radiation coronary computed tomography angiography with low tube voltage and knowledge-based model reconstruction. *Sci. Rep.* **9**, 1308. https://doi.org/10.1038/s41598-018-37870-3 (2019).
18. Hara, A. K. et al. Iterative reconstruction technique for reducing body radiation dose at CT: feasibility study. *AJR Am. J. Roentgenol.* **193**, 764–771. https://doi.org/10.2214/ajr.09.2397 (2009).
19. Leipsic, J., Nguyen, G., Brown, J., Sin, D. & Mayo, J. R. A prospective evaluation of dose reduction and image quality in chest CT using adaptive statistical iterative reconstruction. *AJR Am. J. Roentgenol.* **195**, 1095–1099. https://doi.org/10.2214/ajr.09.4050 (2010).
20. Vorona, G. A. et al. Reducing abdominal CT radiation dose with the adaptive statistical iterative reconstruction technique in children: a feasibility study. *Pediatr. Radiol.* **41**, 1174–1182. https://doi.org/10.1007/s00247-011-2063-x (2011).
21. Prakash, P. et al. Reducing abdominal CT radiation dose with adaptive statistical iterative reconstruction technique. *Invest. Radiol.* **45**, 202–210. https://doi.org/10.1097/RLI.ob013e3181dzfeec (2010).
22. Nievelstein, R. A., van Dam, I. M. & van der Molen, A. J. Multidetector CT in children: current concepts and dose reduction strategies. *Pediatr. Radiol.* **40**, 1324–1344. https://doi.org/10.1007/s00247-010-1714-7 (2010).

Acknowledgements

Not applicable.

Author contributions

Simin Xiao, Conceptualization, Methodology, Data curation, Writing Original draft preparation, Visualization, Software, investigation, writing - review and editing. Siyuan Zeng conceptualization, investigation, writing-review and editing. Yangbin Kou, final approval of the version, writing- review and editing. All authors contributed to the article and approved the submitted version.

Funding

Medical Research Project of Chengdu Municipal Health Commission (Project No. 2022607). Clinical Science Research Fund Project of Chengdu Medical College (Project No. 2022LHZYYB-04). Medical Research Project of Chengdu Municipal Health Commission (Project No. 2024311).

Declarations

Competing interests

The authors declare no competing interests.

Ethics approval and consent to participate

Not applicable.

Consent for publication
Not applicable.

Additional information
Correspondence and requests for materials should be addressed to Y.K.

Reprints and permissions information is available at www.nature.com/reprints.

Publisher's note Springer Nature remains neutral with regard to jurisdictional claims in published maps and institutional affiliations.